# Enhancing Hydrogen Production from Bioenergy Crops via Photoreforming

#Meshal Aljohani[1,2], #Lan Lan[1*], Helen Daly[1*], Pedro Verdía Barbará[3], Min Hu[1], Suhaib Nisar[3], Shengzhe Ding[1], Jason Hallett[3], Neil Watkins[4], William J. Macalpine[5], Rebecca Rowe[6], Agnieszka Brandt-Talbot[7], Gregg Sanford[8], John Ralph[9,10], Shawn D. Mansfield[9,11], Carmine D'Agostino[1,12], Xiaolei Fan[1], Christopher Hardacre[1*]

[1] Department of Chemical Engineering, School of Engineering, The University of Manchester, Manchester, M13 9PL, United Kingdom

[2] Hydrogen Technologies Institute, King Abdulaziz City for Science and Technology (KACST), Riyadh 11442, Saudi Arabia

[3] Department of Chemical Engineering, Imperial College London, London, SW7 2AZ, United Kingdom

[4] Eco Crops Ltd, Cockermouth, CA13 9AN, United Kingdom

[5] Rothamsted Research, West Common, Harpenden AL5 2JQ, United Kingdom

[6] UK Centre for Ecology & Hydrology, Lancaster Environment Centre, Lancaster, LA1 4AP, United Kingdom

[7] Department of Chemistry, Imperial College London, London, W12 0BZ, United Kingdom

[8] Department of Soil & Environmental Sciences, University of Wisconsin-Madison, Madison, WI 53706, United States

[9] DOE Great Lakes Bioenergy Research Centre (GLBRC), Madison, Wisconsin 53726, United States

[10] Department of Biochemistry, University of Wisconsin, Madison, Wisconsin 53706, United States

[11] Department Wood Science and Department of Botany, University of British Columbia, Vancouver, British Columbia, Canada V6T 1Z4

[12] Dipartimento di Ingegneria Civile, Chimica, Ambientale e dei Materiali (DICAM), Alma Mater Studiorum – Università di Bologna, Via Terracini, 28, 40131 Bologna, Italy

[*]Information of corresponding authors can be found in Author Information Notes

#M. A. and L. L. contributed equally to this paper

## Abstract

Photoreforming of perennial bioenergy crops (willow, miscanthus, and poplar) has the potential to generate $H_2$ with reduced environmental impacts. To understand the compositional effects of the biomass on the average rate of $H_2$ production over the first 30 min of reaction ($rH_2$), the $rH_2$ of model biomass component (i.e., cellulose, hemicellulose, and lignin) mixtures were compared with those from the raw biomass. The higher cellulose or hemicellulose content

in multi-component mixtures resulted in higher $rH_2$, whereas lignin reduced hydrogen production rate. However, with raw biomass, the ratio of biomass components alone did not determine the $rH_2$ via photoreforming with rates of hydrogen production for different varieties of willow ranging between 1.9 μmol $h^{-1}$ and 12.3 μmol $h^{-1}$, 11.8 μmol $h^{-1}$ for a poplar, and 6.8 μmol $h^{-1}$ for a miscanthus biomass. In addition, comparable $rH_2$ of raw poplar and its extracted cellulose via an IonoSolv treatment indicated the possibility of using raw biomass materials without delignification for generating $H_2$ via photoreforming. Importantly, the $rH_2$ was positively correlated with the interaction between water and the biomass, as assessed by NMR relaxometry via an examination of the $T_1/T_2$ ratio. A stronger water-biomass interaction resulted in a higher $rH_2$. Genetic modification of biomass has been suggested as a putative way to improve the $rH_2$ of biomass with an enhanced interaction with water. This research enhances the understanding of factors influencing $H_2$ production from lignocellulosic biomass by photoreforming and supports the breeding and management of perennial biomass crops to maximise $H_2$ yields while minimising land area requirements.

**Keywords**: Hydrogen production, bioenergy crops, photoreforming, ionic liquid pretreatment, NMR relaxometry

## Introduction

Lignocellulosic biomass is an abundant renewable resource. Its utilisation is expected to contribute toward minimizing societal dependence on fossil resource-derived energy and materials. Harnessing the energy stored in the chemical bonds of biomass can complement intermittent renewable energy production, while biomass also provides renewable hydrogen and carbon. There is therefore significant interest in the development of biomass conversion technologies to produce energy, biofuels, chemicals, and materials. Hydrogen has an increasing role in sustainable manufacturing as a fuel, an energy storage vector, and as a reagent in many chemical transformations. This has sparked increasing interest in more sustainable means of producing $H_2$. Photocatalytic reforming of lignocellulosic biomass is an approach of growing interest for the sustainable production of $H_2$ in addition to the production of value-added chemicals such as sugars, hydroxymethylfurfural (HMF), and formic acid. It is a light-driven chemical transformation employing a catalyst that generates electron-hole pairs for oxidation and reduction reactions in aqueous solution.[1] The photon energy needed could be sourced from natural sunlight or sustainable artificial light.

The development of catalysts to enhance photocatalytic efficiency has been an area of intense research in photoreforming systems that typically use organic molecules such as alcohols, aldehydes, carboxylic acid, and carbohydrates as the substrate.[2] Raw lignocellulosic biomass is an interesting substrate as it requires minimal pre-conditioning, leading to lower processing costs. However, raw lignocellulosic biomass and its primary polymeric components, cellulose, hemicellulose, and lignin, are more challenging substrates for photoreforming due to their insolubility in water, which limits interaction with catalysts and, due to absorbing/scattering the light, reduces the light available for the photocatalysis. The mechanism and rate of hydrogen production from photoreforming of cellulose and lignin (and related small model compounds such as glucose and aromatics) have been investigated previously.[3] The reforming of isolated lignin substrates has been reported to be slow due to significant absorption of light by the substrate.[4] Higher rates of $H_2$ production have been reported using cellulose.[5] These three biomass components can act as sacrificial agents in photocatalytic hydrogen production [1]. In biomass photocatalysis, photo-excited holes ($h^+$) and electrons ($e^-$) pairs are generated when photocatalysts absorb the photon energy equal to or greater than its band gap energy ($E_{bg}$). Hydrogen can be formed during the reduction of $H^+$ by the $e^-$. Meanwhile, the reactive oxygen species (ROS) such as hydroxyl radicals (·OH) are formed from the reaction between water and $h^+$. The scavenging of $h^+$ can improve the separation of $e^-$-$h^+$ pairs to increase the

efficiency of $H_2$ production. Biomass components undergo oxidation via direct (by $h^+$) and indirect (by ·OH) mechanisms to form reaction intermediates (e.g., glucose and formic acid from cellulose) for further $h^+$ or ·OH scavenging. Additionally, $H_2$ can be produced directly from the protons in biomass via photocatalytic reforming [3a].

$H_2$ production by photoreforming of raw biomass was first demonstrated in 1980 by Kawai et al.[6] and studies using raw biomass to date have predominantly focussed on catalyst development and characterisation and reaction and/or biomass pretreatment conditions (pH, temperature).[7] The various photocatalytic systems (reactor, catalyst, and light sources) were employed but with controversial conclusions on the comparison of $H_2$ production yields and efficiencies from raw biomass substrates to the extracted biopolymers, cellulose or hemicellulose. For example, poplar wood chips have been photoreformed over a 1.0 wt.% $Pt/TiO_2$ catalyst achieving a significantly lower $H_2$ production rate (26 μmol $h^{-1}$ $g_{cat}^{-1}$) compared to α-cellulose (275 μmol $h^{-1}$ $g_{cat}^{-1}$) whereas comparable $H_2$ production rates were reported from cellulose and aspen wood over a Cu/In-doped ZnS catalyst fabricated from the ZIF-8 precursor (74 μmol $h^{-1}$ $g_{cat}^{-1}$)[7c] and from cellobiose and poplar powder over a 1%Pt/$C_3N_4$ (73 and 83 μmol $h^{-1}$ $g_{cat}^{-1}$ respectively).[7d] The current understanding of biomass photoreforming does not allow assessment of the most efficient raw biomass feedstock to produce $H_2$ or whether raw biomass is indeed a viable feedstock compared to the extracted biopolymers, cellulose or hemicellulose.

In this study, willow, poplar, and miscanthus were selected and studied as representative biomass resources for their ability of producing hydrogen via photoreforming. Short-rotation coppice (SRC) willow is a perennial UK biomass crop with rapid growth and short harvest cycles, providing high yield per unit area of land with minimal fertiliser input,[8] characteristics also shared by the biomass crops poplar and miscanthus.[8] These crops are currently predominantly used for the generation of heat and electricity;[9] however, screening crops for their activity in biomass conversion technologies could inform varietal crop choices for landowners/growers by linking crop choice to the yield of the product (such as $H_2$) from the conversion process alongside land-use considerations.

Herein, an initial step in assessing the variability in $rH_2$ by photoreforming of bioenergy crops willow, poplar, and miscanthus has been undertaken. In particular, the photoreforming of different varieties and stem age of SRC willows was investigated and this is also the first study to report using a miscanthus feedstock to produce $H_2$ through photoreforming. For poplar, the

effect of genetically engineering one aspect of the lignin structure on the activity of photoreforming was also considered. The $rH_2$ for the biomass was compared to the $rH_2$ for individual polymeric components (cellulose, hemicellulose, and lignin), model mixtures of the polymeric components, and biomass fractionated with the emerging IonoSolv approach that uses low-cost ionic liquid-water mixtures to generate a cellulose pulp and a lignin.[10] NMR relaxometry was used to measure the interaction strength between the water molecules and the biomass solids. A correlation between the $rH_2$ and the interaction strength between water and biomass was established based on the NMR relaxometry study.

## Results and Discussion

*Comparison of hydrogen production rates of raw willow vs pure biomass components*

Photoreforming reactions in this study were performed over a solid 0.2 wt.% $Pt/TiO_2$ catalyst (preparation and characterisation are presented in the **Supporting Information**, **SI**) that has previously been shown to be effective for a wide range of substrates.[4,5] The average rate of $H_2$ production over the first 30 min of reaction ($rH_2$, recorded during the first 30 min of irradiation) was used as an indicator for activity; time courses for $H_2$ and $CO_2$ production are shown in **Figure S1**. Reactions were performed in water (pH = 7.6) at 35±2 °C. It should be noted that the temperature in the reactor under prolonged UV-LED irradiation increased from an initial temperature of 25-30°C. These mild conditions did not induce degradation/depolymerisation of the biomass allowing comparison of the reactivity of the solid biomass particles with the component biopolymers, cellulose, hemicellulose, and lignin.

Initially, the $rH_2$ for commercially obtained isolated lignocellulosic components hemicellulose, (HC, xylan from beech wood), microcrystalline cellulose (C, from cotton linters), and organosolv lignin (L, extracted from *Platycodon grandiflorum*) were compared. The $rH_2$ for hemicellulose was higher than cellulose at 37.0 and 28.8 μmol $h^{-1}$ (**Figure 1a**), respectively. Although both components are carbohydrate polymers, hemicelluloses possess shorter chain lengths (50-200 sub-units),[11] have lower molecular weights, are often branched, and are amorphous, whereas cellulose is highly crystalline and fibrillar (5,000-10,000 subunits for cellulose in natural biomass),[11] which likely accelerates the photoreforming reaction of hemicellulose compared to cellulose.[12] In contrast, a very low $rH_2$ of 0.7 μmol $h^{-1}$ was observed for the photoreforming of organosolv lignin in agreement with previous studies.[5b] Lignin is a phenylpropanoid polymer and is fundamentally different from cellulose and

hemicellulose. The same order was observed for the $CO_2$ production rate ($rCO_2$): hemicellulose (13.6 μmol $h^{-1}$) > cellulose (11.2 μmol $h^{-1}$) > organosolv lignin (1.1 μmol $h^{-1}$) with similar $H_2$:$CO_2$ ratios observed for hemicellulose (2.7) and cellulose (2.6).

The impact of biomass variability on $rH_2$ was investigated using Salix (willow), a diverse and adaptable genus utilised in the UK. Willow cultivars with different stem ages (1-5 years) grown under a variety of conditions (North and South England) (details provided in **Table 1** and **SI**) were selected as representative biomass samples and their biopolymer component composition was determined using a standard compositional analysis.

***Table 1:*** Details of willow biomass used in this study

| Willow variety | Sample code | Stem age at harvest (years) | Harvesting method | Compositional analysis[a] | | |
|---|---|---|---|---|---|---|
| | | | | %HC | %C | %L |
| Roth Cheviot | W1 | 1 | chipped* | 15.8 | 39.6 | 27.3 |
| Tordis | W2 | 1 | cut stems | 16.6 | 38.6 | 36.6 |
| Tordis | W3 | 3 | cut stems | 19.1 | 51.6 | 28.9 |
| Tordis/Tora | W4 | 5 | cut stems | 19.5 | 49.7 | 26.0 |
| Mixed variety | W5 | >3 | chipped* | 18.9 | 45.5 | 30.7 |

[a] Compositional analysis performed by a standard method published by the National Renewable Energy Laboratory (NREL) Version 54 (NREL/TP-510-42620).[13] Details of compositional analysis procedure can be found in the SI and in the literature.[14] Detailed data for compositional analyses are shown in Table S2. %Hemicellulose (%HC): sum of xylan, galactan, arabinan, and mannan content; %Cellulose (%C): sum of glucan content (glucan was equated to cellulose content); and %Lignin (%L): sum of acid-soluble and acid-insoluble lignin content. *Note, the storage time of chipped willow samples was not recorded, but cell wall materials are generally considered to be quite stable.

The $rH_2$ varied across the willow samples (**Figure 1b**), with the lowest $rH_2$ observed for W1 and the highest $rH_2$ for W5 at 1.9 μmol $h^{-1}$ and 12.3 μmol $h^{-1}$, respectively. The $rH_2$ for the willows was lower than achieved for the polysaccharide components C and HC (**Figure 1a** and **1b**), even for the most reactive willow sample, W5; however, all willows had higher $rH_2$ than the organosolv lignin (0.7 μmol $h^{-1}$) (**Figure 1a** and **1b**).

The difference in $rH_2$ of these willow samples was not related to the biomass preparation procedure (harvesting method, drying, and grinding). For example, the willows with the smallest and highest $rH_2$, W1 and W5, were chipped at harvest, whereas the other willow samples were cut and stored as stems; however, it should be noted that all willows were also ground and sieved to size <180 μm (as shown in **Table S1**) prior to the reactions. There was

also no effect on $rH_2$ because of the moisture content of the biomass when comparing air-dried (moisture content around 9% for all willows) or oven-dried biomass (at 80 °C for 48 h, **Table S1**). The effect of biomass particle size range on photoreforming activity was also studied for the most active willow, W5 (**Table S1**). No significant effect on the $H_2$ production with the size of biomass particles was found when varying the size from 180 µm to 1.8 mm, suggesting that grinding to very small particle size is not needed.

The biopolymer composition of the willow also did not correlate with the photoreforming activity (**Figure S2a** and **S2b**). The hemicellulose content of all the willow samples was roughly similar at 15.8 – 19.5% (**Table 1**), whereas the cellulose (39-52%) and lignin content (27-37%) showed more variation across the willow samples. For example, the cellulose content of W4 was higher than the lignin content (**Table 1**), but the $rH_2$ was like the one observed for W2 that had comparable lignin and cellulose contents. The lack of expected correlation between carbohydrate content and photoreforming suggests that additional factors such as the distribution of biopolymers within the cell wall could be related to the observed differences in $rH_2$ for the willows.

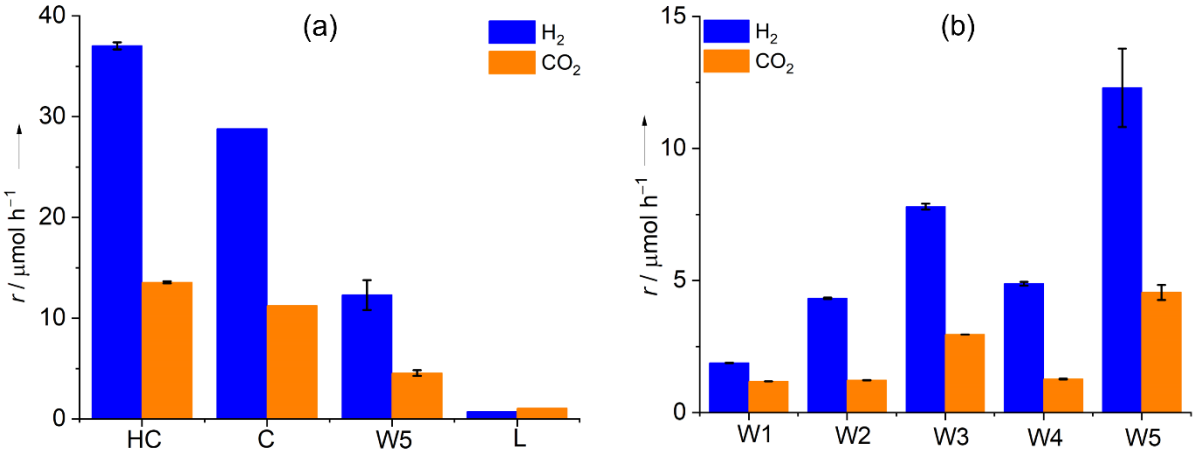


***Figure 1.*** The average rates of gas production over first 30 min reaction (*r*) obtained from photoreforming of (a) willow of different varieties: W1, 1-year-old Roth Cheviot willow; W2, 1-year-old Tordis willow; W3, 3-year-old Tordis willow; W4, Tordis/Tora 5-year-old and W5, mixed variety willow chips harvested at >3 years old. and (b) pure substrates (hemicellulose, HC; cellulose, C; organosolv lignin, L). Reaction conditions: 1 g $L^{-1}$ 0.2 wt.% $Pt/TiO_2$ catalyst and 1 g $L^{-1}$ substrate in 30 mL water under UV-LED irradiation ($I$ = ~43 mW $cm^{-2}$) at room temperature. The range for data point obtained with duplicate experiments is shown as the error bars. The error bars for cellulose and lignin samples were similar as that for hemicellulose.

*Photoreforming of multi-component model mixtures*

Multi-component model mixtures were prepared by mixing hemicellulose, cellulose, and lignin in different ratios (**Table 2**) to assess the competitive reactivity of biomass components when present together in aqueous suspension. The $rH_2$ for component mixtures with different content of hemicellulose, cellulose, and lignin was also examined (**Table 2**). The $rH_2$ for samples with a cellulose content fixed at 25 wt.%, but varying hemicellulose and lignin contents showed a significant reduction in $rH_2$ when the amount of lignin was higher. The $rH_2$ was 21.9 μmol $h^{-1}$ for M1 (25 wt.% C + 55 wt.% HC + 20 wt.% L) and 8.1 μmol $h^{-1}$ for M3 (25 wt.% C + 20 wt.% HC + 55 wt.% L). When the amount of lignin in the reactor was fixed at 35 wt.% and the cellulose to hemicellulose ratio was varied (i.e., M2: with 35 wt.% L + 45 wt.% C + 20 wt.% HC or in M4: 20 wt.% C and 45 wt.% HC), there was only a small difference in the $rH_2$ at 13.7 μmol $h^{-1}$ and 17.3 μmol $h^{-1}$, respectively. Although both hemicellulose and cellulose have shown activity for $H_2$ production under photoreforming conditions, no correlation was observed between the $rH_2$ and the amount of hemicellulose or cellulose separately (**Figure S3**). However, when considered together, a correlation between the amount of lignin in the reactor and $rH_2$ was observed with increasing lignin content reducing the amount of $H_2$ produced (**Figure S4a**). A similar trend was observed for $CO_2$ production, as shown in **Figure S4b**. The chromophoric functionalities in lignin can absorb light of wavelength above 300 nm, leading to a reduction in light absorption by the photocatalyst and therefore reducing the activity of $H_2$ production [3b]. Additionally, during the lignin photoreforming process, the intermediates such as benzoquinone and catechol formed via the aromatic oxidation pathway can poison the photocatalyst by strong adsorption and electron transfer reactions which reduce the $H_2$ formation on the catalyst [3b].

***Table 2:*** The content of cellulose, hemicellulose, and lignin in the multi component mixtures and their average $H_2$ production rate during the first 30 min by the irradiation of UV-LED ($rH_2$, μmol $h^{-1}$) and production yield during irradiation with UV-LED for 2 h. Reaction conditions: 1 g $L^{-1}$ catalyst and 1 g $L^{-1}$ substrates in 30 mL water with irradiation of UV-LED ($I$ = ~43 mW $cm^{-2}$) at room temperature. The range for data point obtained with duplicate experiments is shown as the error bars in the table.

| Mixture | HC (%) | C (%) | L (%) | Average rate of $H_2$ production ($rH_2$, μmol $h^{-1}$) | $H_2$ production yield (μmol) |
|---|---|---|---|---|---|
| M1 | 20 | 25 | 55 | 8.1 ± 0.3 | 19.9 |
| M2 | 20 | 45 | 35 | 13.7 ± 0.3 | 32.0 |
| M3 | 55 | 25 | 20 | 21.9 ± 0.3 | 44.9 |
| M4 | 45 | 20 | 35 | 17.3 ± 0.3 | 34.5 |

| | | | | | |
|---|---|---|---|---|---|
| M5 | 21 | 36 | 43 | 13.4 ± 0.3 | 27.0 |
| M6 | 20 | 42 | 38 | 17.1 ± 0.3 | 37.4 |

The content of sugars and short chain acids in the liquid phase after the photoreforming reaction of M1 and M2 was also determined (**Table S3**) and compared with that from the pure components. For pure cellulose and hemicellulose, sugars and short chain carboxylic acids (formic and acetic acid) were observed, whereas aromatic compounds (eluting at longer retention times) were the only liquid-phase products observed after photoreforming of lignin, as might be expected. In the multicomponent mixtures, the marker compounds (the compound which is observed uniquely in the liquid products of the photoreforming of each biopolymer, i.e., acetic acid for C, formic acid for HC, and aromatic species for L) were observed, indicating conversion of each biopolymer. Conversely, lignin marker compounds were not observed in the liquid phase when raw biomass (W5 willow) was used, indicating the importance of the biomass structure (biopolymer arrangements and accessibility) in its photoreforming activity. This observation coupled with the fact that the mixed willow (W5) gave the highest $r\mathrm{H_2}$ suggests preferential photoreforming of the cellulose and hemicellulose within the raw biomass. This implies that the accessibility of the cellulose and hemicellulose to the OH radicals generated via the photocatalysis is an important factor in biomass photoreforming and that this varies among raw willow samples.

*Photoreforming of miscanthus and poplar bioenergy crops compared to willow*

The $r\mathrm{H_2}$ from the willows (milled and pre-dried) indicate that lignocellulosic biomass without chemical pretreatment, for example, may be a viable feedstock for photoreforming. To explore a wider range of bioenergy crops as substrate for photoreforming, the $r\mathrm{H_2}$ for the photoreforming of a miscanthus and a poplar were studied. The sample details of the miscanthus and poplar studied are summarised in the **SI** (Materials and Characterisations).

The measured $r\mathrm{H_2}$ for miscanthus was 6.8 μmol $h^{-1}$ and 11.8 μmol $h^{-1}$ from the poplar (**Figure 2**). The poplar sample generated a $r\mathrm{H_2}$ comparable to the $r\mathrm{H_2}$ observed for W5, the most active willow for photoreforming, whereas the miscanthus sample exhibited 50% of the photoreforming activity of W5. However, the $r\mathrm{H_2}$ for miscanthus was comparable to the average $r\mathrm{H_2}$ of the five willow samples (6.3 μmol $h^{-1}$). Compositional analysis of the biomass samples (**Table S4**) shows no relationship between the cellulose/hemicellulose/lignin content

and $rH_2$ for miscanthus and poplar, equivalent to the lack of correlation observed for willow (**Figure S2**).

*Photoreforming of IonoSolv fractionated bioenergy crops*

Cellulose and lignin present in lignocellulosic biomass can be separated by IonoSolv fractionation (details in Experimental, **SI**), while hemicellulose is hydrolysed using this approach and removed following solubilisation in the ionic liquid. The IonoSolv cellulose pulps contained native crystalline cellulose (cellulose I structure confirmed by XRD analysis, **Figure S5**) and hence are like microcrystalline cellulose but provide a more meaningful comparison to the raw biomass being from wood as opposed to the purified, commercial MCC from cotton linters. The $rH_2$ for the cellulose pulp and lignin obtained using IonoSolv fractionation was compared with the $rH_2$ obtained for willows W1 and W5, which gave the highest and lowest $rH_2$, the raw miscanthus, and the raw poplar (**Figure 2**). The cellulose pulps demonstrated the highest rate of $H_2$ production, with higher values for W5 and W1 willow pulps at 18.7 μmol $h^{-1}$ and 16.7 μmol $h^{-1}$, respectively, and a comparable rate observed for the miscanthus and poplar pulps at ~15 μmol $h^{-1}$. The lignins extracted from the different biomass samples gave low activity for $H_2$ production, with the $rH_2$ production ranging from 1.3 to 2.1 μmol $h^{-1}$, and were comparable to that for organosolv lignin at 0.7 μmol $h^{-1}$. The $rH_2$ for W1, the raw biomass with the lowest photoreforming activity, was comparable to that for the extracted IonoSolv lignin (1.8 μmol $h^{-1}$).

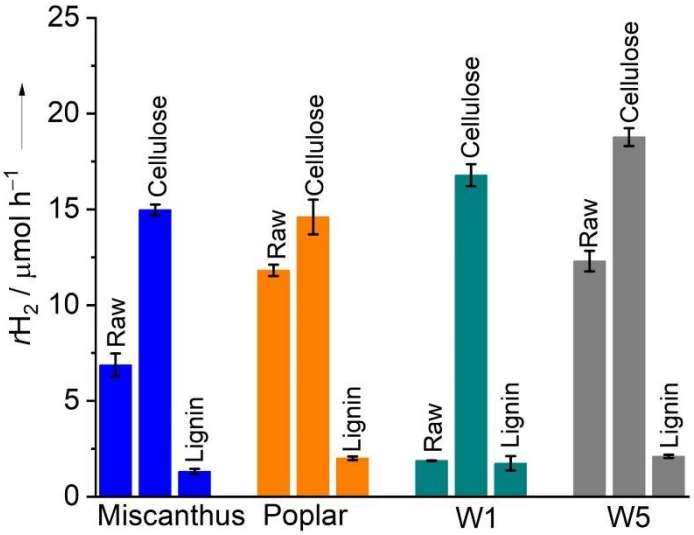


***Figure 2.*** Average $H_2$ production rate over first 30 min reaction ($rH_2$) for the photoreforming of various bioenergy crops (a miscanthus, a poplar, W1 and W5 willows) compared to cellulose pulps and lignins generated by IonoSolv fractionation at 170 °C/45 min for miscanthus and poplar and 150 °C/45 min for the willow biomass. Reaction conditions: 1 g $L^{-1}$ of 0.2 wt.% $Pt/TiO_2$ catalyst, 1 g $L^{-1}$ raw biomass and

pulps, and lignins in 30 mL water under UV-LED irradiation at 35 °C. UV-LED light intensity: $I$ = ~43 mW cm$^{-2}$. The range for data point obtained with duplicate experiments is shown as the error bars in the figure.

The $r$H$_2$ for W1 was comparable to that for the extracted IonoSolv lignin (1.8 μmol h$^{-1}$), whereas the $r$H$_2$ for raw W5 and poplar were more comparable to their IonoSolv cellulose pulps and also had a higher $r$H$_2$ than their respective lignins (**Figure 2)**. The similarity of $r$H$_2$ for W5 and the poplar raw biomass and their respective cellulose pulps (**Figure 2**, poplar and W5 willow) suggests that the H$_2$ production for raw biomass samples could be correlated with the physical properties (morphology, particle size, internal surface area, and porosity) as well as the chemical properties of the biomass (cellulose/hemicellulose/lignin content, localised chemical environment, cellulose crystallinity, hydroxy group content, lignin S/G/H units).[11a] Indeed, the H$_2$ production from W1 being comparable to that from its derived lignin (**Figure 2**, W1) would also suggest that the combined chemical and physical properties of the biomass are important for photoreforming activity.

*Photoreforming of zip-poplar and IonoSolv fractionated Zip-poplar*

A genetically modified "zip-lignin" poplar (labelled Z-Poplar, details in the **SI**) in which the chemical structure of the lignin had been altered to decrease its recalcitrance to hydrolysis without altering the strength and growth of the tree was also employed. The genetic modification has been shown to alter the cellulose at the microfibrillar level, as it was found to be more disorganised compared to the cellulose in unmodified poplar.[15] These modifications in the lignin and cellulose of the engineered poplar could prove beneficial for photoreforming. Z-Poplar cellulose pulps and lignin were also generated via IonoSolv fractionation and compared to the unmodified poplar, as shown in **Figure 3**. Photoreforming experiments showed that the genetic modification did not impact the reactivity of the recovered cellulose and lignin, but did alter the reactivity of the raw biomass, with an H$_2$ yield of 22.3 μmol after 5 h of photoreforming for the Z-Poplar compared to 17.2 μmol for the unmodified poplar (**Figure 3**). The $r$H$_2$ (14.4 μmol h$^{-1}$) and $r$CO$_2$ of raw Z-Poplar had a similar $r$H$_2$ to that of the recovered cellulose pulp ($r$H$_2$, 15.4 μmol h$^{-1}$), as shown in **Figures S6**. The genetic modification on biomass could be a way of improving its reactivity of producing H$_2$ during photoreforming process without extracting out cellulose pulp via IonoSolv fractionation.

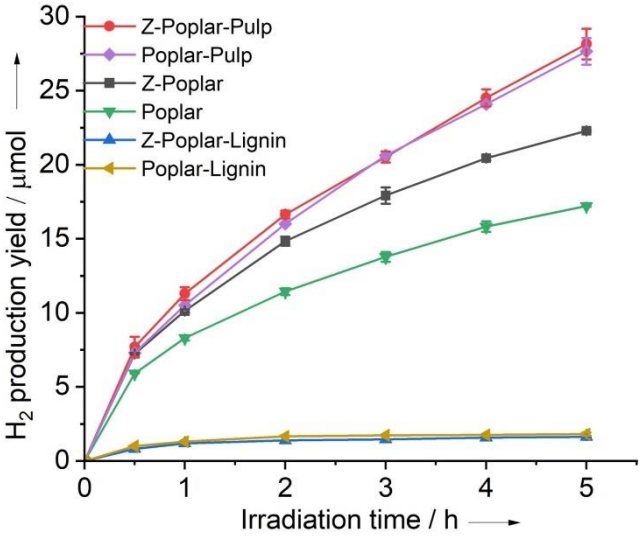


***Figure 3.*** $H_2$ production as a function of reaction time for photoreforming of wild-type poplar and genetically modified poplar compared to cellulose pulps and lignins isolated from both poplars at 170 °C /45 min. Reaction conditions: 1 g $L^{-1}$ catalyst, raw biomass and pulps, and 0.25 g $L^{-1}$ lignin in 30 mL water under UV-LED irradiation at room temperature. UV-LED light intensity: $I$ = ~43 mW $cm^{-2}$. The range for data point obtained with duplicate experiments is shown as the error bars in the figure.

*Effect of interaction between water and substrates*

Lignocellulosic biomass is a hierarchical, porous, anisotropic composite material that can vary with plant species as well as growing conditions.[16] Previous work has shown that the nuclear magnetic resonance (NMR) $T_1/T_2$ relaxation ratio is a robust indicator of surface interactions occurring between a guest molecule and solid surfaces of porous media,[17] and is largely independent of the internal morphology of the porous medium. A recent study demonstrated the usefulness of the method in the study of a biomass material (walnut shells) used for adsorption applications.[18] As mentioned above, the $H_2$ production for raw biomass can be correlated to its physical and chemical properties rather than its bulk composition. The interaction strength of a guest molecule and solid is affected by the physical and chemical properties of the solid surface.[19]

In general, photogenerated electrons ($e^-$) and holes ($h^+$) are formed over the photocatalyst when sufficient photo energy (greater than the bandgap energy of the catalyst) is absorbed by the photocatalyst. In an aqueous system, water is adsorbed on the catalyst and dissociated into $H^+$ and $OH^-$. The $OH^-$ is oxidised by the $h^+$ to form ·OH radicals, while $H^+$ in the system is reduced by the $e^-$ to form $H_2$.[4] *In situ* (photo)hydrolysis of biomass (action of photogenerated $H^+$/·OH) is likely to be promoted in biomass samples in which water has greater mobility/access to the more hydrophilic and reactive biomass components. Water has been identified to play the role

of a proton-conduction medium, able to transport $H^+$;[20] in the autohydrolysis of biomass, $H_3O^+$ (a protonated $H_2O$ molecule) was reported to play a role in the penetration of biomass structure aiding hemicellulose hydrolysis.[21] The mechanism indicates it is the activated water (·OH) that interacts with the solid biomass causing hydrolysis and decomposition to $H_2$. Without this interaction the system (i.e., solid biomass and solid catalysts in an aqueous system) does not operate. The interaction between water molecules and biomass solids was therefore measured to provide the information of this interaction strength affecting on the $rH_2$. Herein, the NMR $T_1/T_2$ ratio was used to probe the interaction strength of water with biomass samples (details can be found in the **SI**) to identify the effect of this interaction on the photoreforming of raw biomass.

The NMR $T_1/T_2$ ratios of water in the lignocellulosic biomass samples are summarised in **Table S5**. As shown in the table, the experimental data fall within two groups of values: a group comprising poplar and W5, showing higher ratios at around 5.7; and the group of miscanthus, W1, W2, W3, and W4 willows showing lower ratios at around 2.5. A clear correlation can be seen (**Figure 4)** between the $T_1/T_2$ values and their initial production rates of $H_2$ from photoreforming. The interaction of water with poplar was increased for the Z-Poplar sample and follows the correlation observed between $rH_2$ and NMR $T_1/T_2$ ratio. With little structural differences between the lignin of the poplar and Z-Poplar, the enhanced $H_2$ production may be attributed to changes in the cell wall porosity and/or modification of the cellulose structure, resulting in improved access/interaction of water.

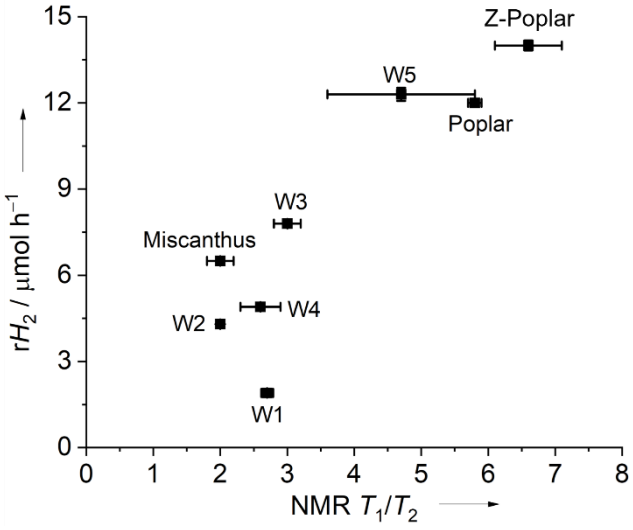


***Figure 4.*** Correlation of NMR $T_1/T_2$ and the average production rates of $H_2$ over the first 30 min reaction ($rH_2$) from the photoreforming of biomass (willow, miscanthus and poplar): W1 – 1-year-old Roth Cheviot willow, W2 – 1-year-old Tordis willow, W3 – 3-year-old Tordis willow, W4 – Tordis/Tora 5-

year-old and W5 – mixed variety willow chips harvested at >3 years old. The standard deviation for data point obtained with repeated experiments (3-4 times) is showed as the error bars in the figure.

The higher NMR $T_1/T_2$ values indicates a higher interaction strength, on average, between water and the biomass. This suggests that photoreforming activity is related to the strength of interaction between water and biomass components. In this context, the NMR results reported in **Figure 4** suggest that water interaction with the substrate plays a key role in determining the reactivity of the system, and NMR relaxation measurements can be used as a predictive indicator for reaction performance. This correlation could be extended to pure components (C and L, as shown in Figure S14, SI), however, the IonoSolv extracted cellulose and lignin samples did not follow the trend for the raw biomass samples. This is thought to be due to residual ionic liquid being present following the IonoSolv treatment.

## Conclusions

Several bioenergy crops, including different varieties of willow and two poplar (wildtype and genetically modified), and one type of miscanthus, were studied as substrates for photoreforming and shown to produce $H_2$. Willow generated $H_2$ at widely varying rates between 1.9 and 12.3 μmol $h^{-1}$, with poplar and miscanthus falling within that range with 11.8 μmol $h^{-1}$ and 6.8 μmol $h^{-1}$, respectively with the Z-Poplar showing highest $rH_2$ of 14.4 μmol $h^{-1}$. Although the $rH_2$ was generally lower for raw biomass than for cellulose or hemicellulose, the raw poplar samples (wild type and poplar with a genetic modification of the lignin) exhibited $rH_2$ approaching those achieved with cellulose pulps obtained with Ionosolv fractionation. The varied $rH_2$ from the photoreforming of raw bioenergy crops highlights the potential benefits from considering conversion activity in conjunction with parameters such as yield per land area in breeding programmes and varietal crop selections. We additionally demonstrate the potential added value of NMR $T_1/T_2$ analysis in screening biomass feedstocks for $H_2$ production as a convenient alternative to calculating the level following a determination of the amount of each of the polymer components in the raw biomass. Assessment of the interaction between water and biomass could be part of a characterisation toolkit of biomass properties, linking to mechanistic insights and photoreforming system optimisation for biomass feedstocks (reactor and catalyst design and light source).

**Acknowledgements**

The authors would like to acknowledge the EPSRC-funded Supergen Bioenergy Hub 2018 (EP/S000771/1) for funding this research and King Abdulaziz City for Science and Technology for financial support for Meshal Aljohani's scholarship. UK Catalysis Hub is kindly thanked for resources and support provided via our membership of the UK Catalysis Hub Consortium and funded by EPSRC grants: EP/R026939/1, EP/R026815/1, EP/R026645/1 and EP/R027129/1. The project has received funding from the European Union's Horizon 2020 research and innovation program under grant agreement No 872102. JR, GRS, and SDM were supported by the Great Lakes Bioenergy Research Center, U.S. Department of Energy, Office of Science, Biological and Environmental Research Program under Award Number DE-SC0018409. The Z-Poplar sample was obtained from the DOE Great Lakes Bioenergy Center at U. Wisconsin-Madison, from field-grown material propagated by Gregg Sanford from materials originally created by Shawn Mansfield's group at University of British Columbia, Canada.

**Author Information Notes**

#Meshal Aljohani and Lan Lan have contributed equally to this work.

*Corresponding authors: lan.lan@manchester.ac.uk; helen.daly@manchester.ac.uk; c.hardacre@manchester.ac.uk

**Associated Content**

Experimental section (Materials and Characterisation; Procedure of Ionosolv Treatment and Characterisations; Photocatalytic Reforming Reaction; Nuclear Magnetic Resonance Spectroscopy NMR $T_1/T_2$ measurements) and supporting tables and figures are included in the Supporting Information (SI)

## References


[1] N. Skillen, H. Daly, L. Lan, M. Aljohani, C. W. J. Murnaghan, X. Fan, C. Hardacre, G. N. Sheldrake, P. K. J. Robertson, Photocatalytic Reforming of Biomass: What Role Will the Technology Play in Future Energy Systems. *Top. Curr. Chem.* **2022**, *380*, 33. DOI: 10.1007/s41061-022-00391-9

[2] a) L. Wang, Z. Zhang, L. Zhang, S. Xue, W. O. S. Doherty, I. M. O'Hara, X. Ke. Sustianable Conversion of Cellulosic Biomass to Chemicals under Visible-light Irradiation. *RSC Advances* **2015**, *5*, 85242-85247. DOI: 10.1039/C5RA16616K; b) H. Kasap, D. S. Achilleos, A. Huang, E. Reisner. Photoreforming of Lignocellulose into $H_2$ Using Nanoengineered Carbon Nitride under Benign Conditions. *J. Am. Chem. Soc.* **2018**, *140*, 11604-11607.DOI: 10.1021/jacs.8b07853; c) H. Fan, G. Li, F. Yang, L. Yang, S. Zhang. Photodegradation of Cellulose under UV Light Catalysed by $TiO_2$. *J. Chem. Technol. Biotechnol.* **2011**, *86*, 1107-1112. DOI: 10.1002/jctb.2632; d) G. Zhang, C. Ni, X. Huang, A. Welgamage, L. A. Lawton, P. K. Robertson, J. T. Irvine, Simultaneous Cellulose Conversion and Hydrogen Production Assisted by Cellulose Decomposition under UV-light Photocatalysis. *Chem. Commun.* **2016**, *52*, 1673-1676. DOI: 10.1039/C5CC09075J

[3] a) L. Lan, H. Daly, R. Sung, F. Tuna, N. Skillen, P. Robertson, C. Hardacre, X. Fan. Mechanistic Study of Glucose Photoreforming over $TiO_2$-based Catalysts for $H_2$ Production. *ACS Catal.* **2023**, 8574-8587. DOI: 10.1021/acscatal.3c00858; b) M. Aljohani, H. Daly, L. Lan, A. Mavridis, M. Lindley, S. Haigh, C. D'Agostino, X. Fan, C. Hardacre. Enhancing Hydrogen Production from the Photoreforming of Lignin. *ChemPlusChem* **2023**, 1-26. DOI: 10.1002/cplu.202300411

[4] a) M. F. Kuehnel, E. Reisner, Solar Hydrogen Generation from Lignocellulose. *Angew. Chem. Int. Ed. Engl.* **2018**, *57*, 3290-3296. DOI: 10.1002/anie.201710133; b) C. Shi, F. Kang, Y. Zhu, M. Teng, J. Shi, H. Qi, Z. Huang, C. Si, F. Jiang, J. Hu. Photoreforming lignocellulosic Biomass for Hydrogen Production: Optimized Design of Photocatalyst and Photocatalytic System. *Chem. Eng. J.* **2023**, 452, 138980. DOI: 10.1016/j.cej.2022.138980

[5] a) L. Lan, Y. Shao, Y. Jiao, R. Zhang, C. Hardacre, X. Fan. Systematic Study of $H_2$ Production from Catalytic Photoreforming of Cellulose over Pt Catalysts Supported on $TiO_2$. *Chin. J. Chem. Eng.* **2020**, 1-8. DOI: 10.1016/j.cjche.2020.03.030 ; b) L. Lan, H. Daly, Y. Jiao, Y. Yan, C. Hardacre, X. Fan. Comparative Study of the Effect of $TiO_2$ Support Composition and Pt Loading on the Performance of $Pt/TiO_2$ Photocatalysts for Catalytic Photoreforming of Cellulose. *Int. J. Hydrogen Energy.* **2021**, 31054-31066. DOI: 10.1016/j.ijhydene.2021.06.043; c) L. Lan, H. Chen, D. Lee, S. Xu, N. Skillen, A. Tedstone, P. Robertson, A. Garforth, H. Daly, C. Hardacre, X. Fan. Effect of Ball-milling Pretreatment of Cellulose on Its Photoreforming for H2. *ACS Sustain. Chem. Eng.* **2022**, 4862-4871. DOI:10.1021/acssuschemeng.1c07301

[6] T. Kawai, T. Sakata, Conversion of Carbohydrate into Hydrogen Fuel by a Photocatalytic Process. *Nature*, **1980**, 286, 474-476. DOI: 10.1038/286474a0

[7] a) Q. Cheng, Y. J. Yuan, R. Tang, Q. Y. Liu, L. Bao, P. Wang, J. Zhong, Z. Zhao, Z. T. Yu, Z. Zou, Rapid Hydroxyl Radical Generation on (001)-Facet-Exposed Ultrathin Anatase $TiO_2$ Nanosheets for Enhanced Photocatalytic Lignocellulose-to-$H_2$ Conversion. *ACS Catal.* **2022**, *12*, 2118-2125. DOI: 10.1021/acscatal.1c05713; b) P. Wang, Y. J. Yuan, Q. Y. Liu, Q. Cheng, Z. K. Shen, Z. T. Yu, Z. Zou. Solar-driven Lignocellulose-to-$H_2$ Conversion in Water Using 2D-2D $MoS_2/TiO_2$ Photocatalysts. *ChemSusChem* **2021**, *14*, 2860-2865. DOI: 10.1002/cssc.202100829; c) H. Nagakawa, M. Nagata. Highly Efficient Hydrogen Production in the Photoreforming of Lignocellulosic Biomass Catalyzed by Cu, In-doped ZnS Derived from ZIF-8. *Adv. Mater. Int.* **2022**, *9*, 2101581. DOI: 10.1002/admi.202101581; d) C. Rao, M. Xie, S. Liu, R. Chen, H. Su, L. Zhou, Y. Pang, H. Lou, X. Qiu. Visible Light-driven Reforming of Lignocellulose into $H_2$ by Intrinsic Monolayer Carbon Nitride. *ACS Appl. Mater. Int.* **2021**, *13*, 44243-44253. DOI: 10.1021/acsami.1c10842

[8] S. Szczukowski, M. Stolarski, J. Tworkowski, J. Przyborowski, A. Klasa. Productivity of Willow Coppice Plants Grown in Short Rotations. *Plant Soil and Environment* **2005**, *51*, 423.

[9] Department of Energy Security and Net Zero, "Digest of UK Energy Statics Annual data for UK, 2023". GOV.UK, https://www.gov.uk/government/statistics/digest-of-uk-energy-statistics-dukes-2024. accessed 2024-07-30

[10] A. Brandt-Talbot, F. J. Gschwend, P. S. Fennell, T. M. Lammens, B. Tan, J. Weale, J. P. Hallett. An Economically Viable Ionic Liquid for the Fractionation of Lignocellulosic Biomass. *Green Chem.* **2017**, *19*, 3078-3102.DOI: 10.1039/C7GC00705A

[11] a) A. Zoghlami, G. Paes. Lignocellulosic Biomass: Understanding Recalcitrance and Predicting Hydrolysis. *Front. Chem.* **2019**, *7*, 874. DOI: 10.3389/fchem.2019.00874; b) T. Heinze, O. A. El Seoud, A. Koschella, *Cellulose derivatives: synthesis, structure, and properties*, Springer, **2018**; c) P. Sharma, C. Bhandari, S. Kumar, B. Sharma, P. Bhadwal, N. Agnihotri, Chapter 11 – Dietary Fibers: A Way to a Healthy Microbiome, in *Diet, Microbiome and Health*, Elsevier, **2018**, pp. 299-345. DOI: 10.1016/B978-0-12-811440-7.00011-9

[12] X. Xu, L. Shi, S. Zhang, Z. Ao, J. Zhang, S. Wang, H. Sun. Photocatalytic Reforming of Lignocellulose: A Review. *Chem. Eng. J.* **2023**, 143972. DOI: 10.1016/j.cej.2023.143972

[13] A. Sluiter, B. Hames, R. Ruiz, C. Scarlata, J. Sluiter, D. Templeton, D. Crocker. Determination of Structural Carbohydrates and Lignin in Biomass. *Laboratory Analytical Procedure* **2008**, *1617*, 1-16.

[14] F. J. Gschwend, F. Malaret, S. Shinde, A. Brandt-Talbot, J. P. Hallett. Rapid Pretreatment of Miscanthus Using the Low-cost Ionic Liquid Triethylammonium Hydrogen Sulfate at Elevated Temperatures. *Green Chem.* **2018**, *20*, 3486-3498. DOI: 10.1039/C8GC00837J

[15] W. Shen, C. Collings, M. Li, J. Markovicz, J. Ralph, S. D. Mansfield, S. Y. Ding. Imaging Changes in Cell Walls of Engineered Poplar by Stimulated Raman Scattering and Atomic Force Microscopy. *ACS Sustainable Chemistry & Engineering* **2019**, *7*, 10616-10622. DOI: 10.1021/acssuschemeng.9b01166

[16] a) D. Sawada, U. C. Kalluri, H. O'Neill, V. Urban, P. Langan, B. Davison, S. V. Pingali. Tension Wood Structure and Morphology Conducive for Better Enzymatic Digestion. *Biotechnology for biofuels* **2018**, *11*, 1-9. DOI: 10.1186/s13068-018-1043-x; b) N. J. Brereton, M. J. Ray, I. Shield, P. Martin, A. Karp, R. J. Murphy. Reaction Wood- A Key Cause of Variation in Cell Wall Recalcitrance in Willow. *Biotechnology for biofuels* **2012**, *5*, 1-11. DOI: 10.1186/1754-6834-5-83; c) N. Berthod, N. J. Brereton, F. E. Pitre, M. Labrecque. Five Willow Varieties Cultivated Across Diverse Field Environments Reveal Stem Density Variation Associated with High Tension Wood Abundance. *Frontiers in plant science* **2015**, *6*, 948. DOI: 10.3389/fpls.2015.00948; d) B. Kulig, E. Gacek, R. Wojciechowski, A. Oleksy, M. Kołodziejczyk, W. Szewczyk, A. Klimek-Kopyra. Biomass Yield and Energy Efficiency of willow depending on cultivar, harvesting frequency and planting density. *Plant, Soil & Environment* **2019**, *65*, 377-386

[17] a) C. D'Agostino, J. Mitchell, M. D. Mantle, L. F. Gladden. Interpretation of NMR Relaxation as a Tool for Characterising the Adsorption Strength of Liquids inside Porous Materials. *Chem. Eur. J.* **2014**, *20*, 13009-13015. DOI: 10.1002/chem.201403139; b) N. Robinson, P. Bräuer, A. P. York, C. D'Agostino. Nuclear Spin Relaxation as A Probe of Zeolite Acidity: A Combined NMR and TPD Investigation of Pyridine in HZSM-5. *PCCP* **2021**, *23*, 17752-17760. DOI:10.1039/D1CP01515J

[18] M. R. Barr, L. Forster, C. D'agostino, R. Volpe. Alkaline Pretreatment of Walnut Shells Increases Pore Surface Hydrophilicity of Derived Biochars. *Appl. Surf. Sci.* **2022**, *571*, 151253. DOI: 10.1016/j.apsusc.2021.151253

[19] Y. Xiao, S. Li, J. Xu, F. Deng. Solid-state NMR Studies of Host-guest Chemistry in Metal-organic Frameworks. *Current Opinion in Colloid & Interface Science* **2022**, *61*, 101633 DOI: 10.1016/j.cocis.2022.101633

[20] G. L. Chiarello, D. Ferri, E. Selli. Effect of the $CH_3OH/H_2O$ Ratio on the Mechanism of the Gas-phase Photocatalytic Reforming of Methanol on Noble Metal-modified $TiO_2$. *J. Catal.* **2011**, *280*, 168-177. DOI: 10.1016/j.jcat.2011.03.013

[21] M. E. Vallejos, F. E. Felissia, M. C. Area. Hydrothermal Treatments Applied to Agro- and Forest-industrial Waste to Produce High Added-value Compounds. *Bioresources* **2017**, 12, 1, 2058-2080.

## TOC Graphic

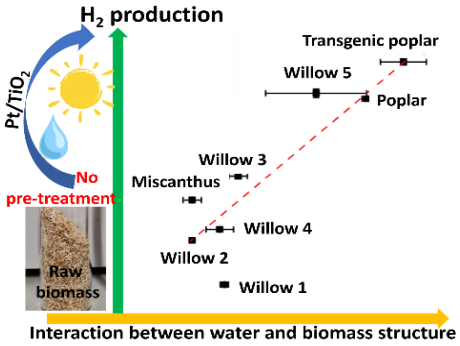
H2 production
Transgenic poplar
Willow 5
Poplar
Pt/TiO2
No
pre-treatment
Willow 3
Miscanthus
Willow 4
Willow 2
Raw
biomass
Willow 1
Interaction between water and biomass structure